STUDY MAGNETIC ELECTRON SCATTERING FORM FACTOR OF ^{24}Mg ISOTOPE

Khelfa Fadel SHEDHAN

1Directorate General of Education in Babylon Governorate, Iraq

Haneen Waheed KADHIM

Al-Qasim Green University, Iraq

Mohammed Yahya HADI[1]

Al-Qasim Green University, Iraq

Abstract

The magnetic form factor of ^{24}Mg isotope under inelastic electron scattering was subjected to computational scrutiny via the utilization of the Oxbash code. The endeavor involved elucidating energy levels intrinsic to this nucleus through the application of the shell model, wherein the model space encompassed zbm, psd, spsdpf, and sd configurations. In the context of the sd model, the investigation harnessed two pioneering USD-type Hamiltonians, denoted as USDC and USDI, in conjunction with tailored amendments to these interaction potentials, referred to as USDCm and USDIm. This study culminated in comprehensively juxtaposing all computational outputs with empirical data sources, including information extracted from the National Nuclear Data Center (NNDC) repository. Significantly, this systematic examination underscored a notable congruence between the derived computational outcomes and the empirical observations. This alignment became conspicuously pronounced subsequent to judicious adjustments made to the g-factors, specifying values of g_l^p = 1.060 and g_l^n = -0.060. The profound unity between the findings of this study and experimental data manifests as compelling evidence, substantiating the efficacy and precision of the employed interaction models. It implies a reliable capacity of these models in the precise computation of magnetic form factors M1, M2, and M3.

Keywords: *Magnetic form factor, USD Hamiltonian, Effective Interaction, Excited States and Transitions Probability.*

Introduction

The shell model plays a central role since it is built on the fewest assumptions possible. It is also critical to appreciate that the shell model has successfully described light nuclei at low excitation energies [1]. Many people still apply the nuclear shell model in atomic theory. Quantitative knowledge can be obtained by employing this procedure. However, it can also be used as a starting point for more complex and complete computations. Residual interaction among valence nucleons is significant, and a shell model is widely regarded as the most fundamental model. As with the distribution of charge and nuclear size and size of nuclei, the distribution of electrons is affected by both charge and size. In general, charge and current density have a dramatic effect on electron scattering [2]. For the nuclear shell model to be successful, the two-body effective interaction is essential. It determines the correctness of shell-model calculations that assume a suitable core to be inert and a limited amount of available space, and this space occupied by residual particles called valance particles [3]. Many ways have been employed to determine the nuclear state's energy accurately[4]–[6]. Then, calculating other observable values is available under that calculation. Although the shell-model codes typically provide 1 KeV of numerical accuracy, the shell-model configuration mixing is the most effective way to achieve this objective [7]. The matrix is built on all possible Slater determinants in this method, with diagonalization limited to a small subset of valence orbits. A set of single-particle energies (SPEs) and two-body interaction matrix elements or two-body matrix elements are required for the shell-model configuration mixing calculations (TBME). These sets are now known as effective interaction or model space Hamiltonian sets. Hamiltonian's model space can be represented in two ways: the first is the "realistic" technique, which is built for a given shell model space from known data on the free nucleon-nucleon force. The second method is "empirical," and it is based on parameters whose values are derived by the agreement between shell model eigenvalues and measured level energies [8][9].

The study magnetic electron scattering form Factor of some isotopes with Z = N have attracted significant attention in various shell-model computations [10][11][12]. The importance of these nuclei arises from the study of pairing interactions between fermions and the excited states (E.S.), which could be isoscalar (isospin T) with T = 0 or isovector with T= 1. The study of these (E.S.) is an effective approach to understand the behavior of many-body quantum systems. ^{24}Mg nucleus is one of these nuclei with unique features and has a sufficient number of nucleons for shell-model calculations and the manifestation of collective excitations associated with massive, prolate deformations [13]. In the case of ^{24}Mg, the atomic numbers are Z = 12 and N = 12. It is an excellent testing ground for microscopic descriptions of unusual nuclei with a shell structure based on cross-shell configurations. Using the shell model, it becomes much easier to differentiate between the (E.S.) in the main valence sd shell for the positive-parity states, and the (E.S.) of the negative-parity states with invader excitations in the zbm, psd, and spsdpf shells.

Negative-parity states, referred to as exotic states, arise as a result of one nucleon being promoted from the p to sd shell for nuclei near ^{16}O or from the sd to fp shell for nuclei near ^{40}C. The ^{24}Mg nucleus is located in the center of the sd shell, where the two types of transitions compete. Despite a wealth of experimental evidence, few theoretical analyses have been undertaken on these nuclear states designated for certain angular momentum J values [14].

In this work zbm, psd, sd, and spsdpf space models were used to calculate the magnetic electron scattering (M_L) form factor for ^{24}Mg and compare all results with the available experimental data.

1. Theory

The interaction of electrons with nuclei's spin and current distributions may be considered an exchange of a virtual photon with angular momentum (±1) traveling in the direction of momentum transfer q. This is referred to as transverse scattering. According to the parity and angular momentum selection criteria, only electric multipoles may have longitudinal components. In contrast, electric and magnetic multipoles can have transverse components. The squared magnetic form factors (ML) for electron scattering between nuclear states J_i and J_f involving angular momentum transfer J are given by [15][16]

$$\left|F_J^m(q)\right|^2 = \frac{4\pi}{z^2}\frac{1}{2J_i+1}\left|\sum_T (-1)^{T_f-T_z}\begin{pmatrix} T_f & T & T_i \\ -T_z & 0 & T_z \end{pmatrix}\langle\Gamma_f\|\hat{T}_\Gamma^m(q)\|\Gamma_i\rangle\right|^2$$
$$\left|\exp\left[-\frac{1}{4}\left(0.43 - \frac{b^2}{A^2}\right)q^2\right]\right|^2$$

(1)

The exponential factor compensates for the nucleon's limited size and the center of mass motion. In coordinated space and isospace, Greek symbols are employed to represent quantum numbers i.e., $\Gamma_i \equiv J_iT_i$, $\Gamma_f \equiv J_fT_f$, and $\Gamma \equiv JT$. While Z, A, and b are atomic number, the mass number, and the size parameter, respectively [17].

Types of electron-scattering form factors are $longitudinal\ F(CL, q, f, i)$, and transverse which have two types $magnetic\ F(ML, q, f, i)$ & $electric\ F(EL, q, f, i)$ where L is the multipolarity. The total transverse form factors given by [18] :

$$F_T^2(q, f, i) = \sum[F^2(EL, q, i, f) + F^2(ML, q, i, f)]$$ (2)

It is clear from Eq. (2) that it consists of two parts, the first being the electrical form factors $F^2(EL, q, i, f)$ and the second referring to the magnetic form factors $F^2(ML, q, i, f)$, which will restrict to a study in this paper. The transverse form factor has two components, one results due to the orbital motion of the nucleon called convection currents (Lc), and the other from intrinsic magnetic moments of the nucleons named magnetization currents (Lm)[19][15]. Therefore, based on what has been explained, the formulas can be written in the following form:

$$F(EL, q, f, i) = F(EL_c, q, f, i) + F(EL_m, q, f, i)$$ (3)

$$F(ML, q, f, i) = F(ML_c, q, f, i) + F(ML_m, q, f, i) \quad (4)$$

The final expression of form factor is given by [20]

$$F(XL, q, f, i) = \frac{4\pi^{1/2}}{Z(2J_I+1)} G_{cm}(q) \sum_{t_z, x} w_{fs}(XLx, q, f, i, t_z) \quad (5)$$

Where $G_{cm}(q) = e^{(b^2 q^2/4A)}$ represents the center of mass correction and, (b) is the harmonic oscillator size parameter, A is the mass number .The symbol x describes the convection (c) and magnetic current (m).here will study the magnetic part from the transvers form factor therefore Eq.(5) write as[20]:

$$F(ML, q, f, i) = \frac{4\pi^{1/2}}{Z(2J_I+1)} G_{cm}(q) \sum_{t_z, x} w_{fs}(MLx, q, f, i, t_z) \quad (6)$$

$w_{fs}(MLx, q, f, i, t_z)$ represent the elements of the reduced matrix. It is found by relying on the limited size of the nucleon. These matrix elements are calculated from

$$w_{fs}(MLx, q, f, i, t_z) = w(MLx, q, f, i, t_z) \frac{g_{fs}(Mx, q, t_z)}{g(Mx, t_z)} \quad (7)$$

$w(MLx, q, f, i, t_z)$ the nucleon reduced matrix elements,

t_z proton or neutron isospin [18].

$g(Mx, t_z)$ free nucleon g factors where Mx at $x = c \rightarrow Mc; g(Mc, t_z) = g_l(t_z)$ and Mx at $x = m \rightarrow Mm; g(Mm, t_z) = g_s(t_z)$. The parameters $g_{fs}(Mx, q, t_z)$ are the empirically determined [21] equivalent q-dependent form factors for unbound nucleons. The form factors of multi particles given by:

$$w(ML, q, f, i, t_z) = \sum_{a,b} \text{OBDM}(L, a, b, f, i, t_z) w(ML, q, a, b, t_z) \quad (8)$$

The configuration mixing is described in terms of the components of the $\text{OBDM}(L, a, b, f, i, t_z)$ One Body Density Matrix multiplied by the elements of the single-particle matrix, *a,b* are the quantum numbers in the initial and final states. The integrals of the multiple relevant operators over the nucleon coordinates $\vec{r}$ yield the reduced single-particle form factors $w(ML, q, a, b, t_z)$ given as [18]:

$$w(MLc, q, a, b, t_z) = \int \langle a, t_z \| \vec{M}(Lc, q, \vec{r}) \cdot \vec{J}_{t_z}(c, \vec{r}) \| b, t_z \rangle d^3 r \quad (9)$$

$$w(MLm, q, a, b, t_z) = \int \langle a, t_z \| \vec{M}(Lm, q, \vec{r}) \cdot \vec{J}_{t_z}(m, \vec{r}) \| b, t_z \rangle d^3 r \quad (10)$$

The shell model was calculated with the assumption that the nucleus consists of a core and valence nucleons. Because the core is inactive, only the mobility of the valence nucleons in the shell model space needs to be taken into account. Theoretically, it is possible to demonstrate that the consequences of virtual excitations of nucleons from core shells into higher orbits are significant. To account for model-space truncation effects, the effective charges and g factors might be used. In shell-model computations, the effective charges and

g factors are frequently employed as an approximation in the renormalization of the single-particle matrix components[22].

2. Results and Discussions

Nuclear scientists use the theory of shell model to calculate and measure the energy levels of medium and heavy nuclei to solve one of the most difficult nuclear physics problems. In this regard, it is necessary to check the computer codes used and their realism. In this paper, the calculations were made with the help of the OXBASH code for Windows [23]. This computer program is effective in calculating the energy levels of light and medium nuclei. By using it, were able to measure the energy levels of the nucleus and conduct a scientific study of the results [24].

The magnesium nucleus ^{24}Mg was used in this research, which has an equal amount of protons and neutrons(Z=N). The phenomenon of electron scattering, which acts as a probe to compute and analyze the size of the nucleus, was used to explore the magnetic electron scattering form factor and energy levels. During an electromagnetic interaction, electron scattering occurs, and studies in this area establish the nucleus's so-called electromagnetic structure. We demonstrate in this article that the study did not depend only on the sd model space, as has been the case in most previous studies, where most scholars [3], [7], [11], [25]–[27], especially when investigating this structure, relied primarily on the sd model space.

There were four parts to the computations. in the first computations assumption, the space model consists of an inert core represented by ^{4}He, has 20 valence particles dispersed throughout the model space of the psd, dependent on the effective interaction of the PSDMWK. The effective model space of the zbm was taken with an inert core of ^{12}C and 12 valence particles dispersed throughout the model space of $(p_{1/2} \, d_{5/2} \, s_{1/2})$, and the effective interaction was taken as REWIL, The space of the model spsdpf was added as it is without inert core and the effective interaction used WBT. the space of the last model was sd which insert new four Hamiltonian were introduced USDC, USDCM, USDI, USDIM [27] in addition to the interaction USDB[29], and W effective interaction, then compared theoretical results between them and the practical values available.
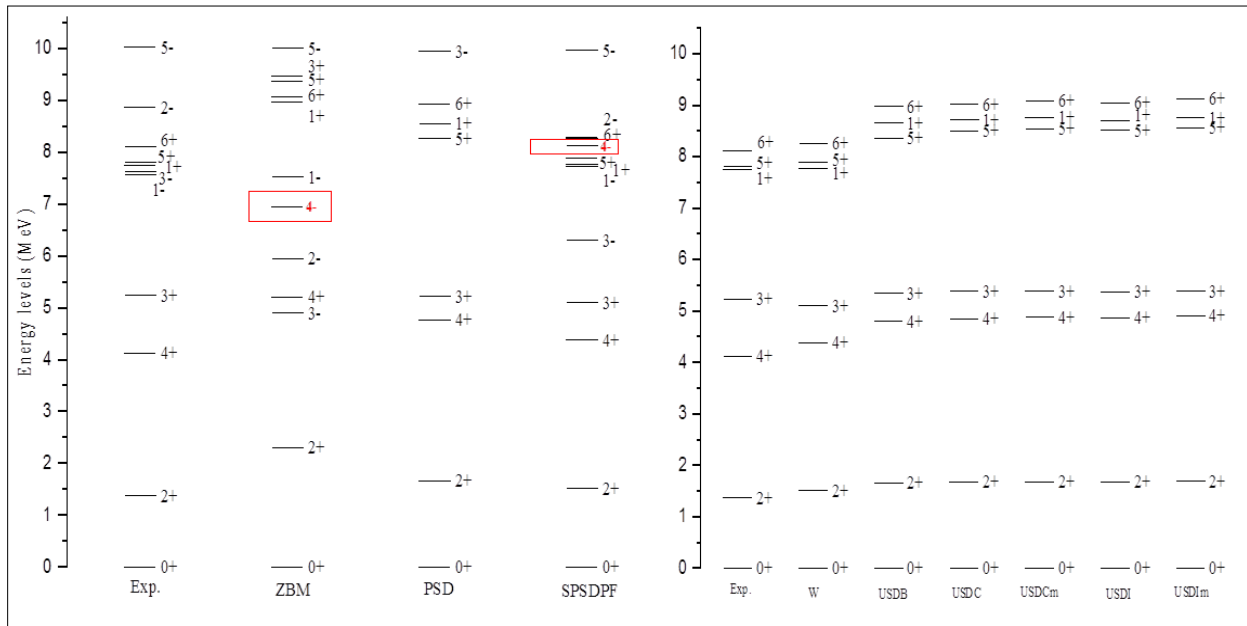
a. Energy levels

The Magnesium ^{24}Mg valence particles have the advantage of occupying a wider model space than sd space, where they can occupy the sdpf model space, or space can be considered as psd if the core adopts a helium ^{4}He, on the other hand, all particles of this nucleus can be considered as valence particles that occupy all possible space inside it, in this case, can use the space of the spsdpf model, that means the inert core of nucleus is neglected "not exist". In this case, valence particles can make a large number of possible formations in these spaces but will face the obstacle of long calculations and the need large storage space, so the number of particles that can exist should constraint in a wider model area by using the constraints which provided by the OXBASH program [14][18].

The ground states (G.S.) wave function of the sd, zbm, psd, spsdpf space model, were calculated at this work, and it was noted that it agrees well with the available experimental data[30]. Fig. (1) indicates the energy levels within the first sequence only, and it was seen that the theoretical and practical data are very close, in addition to the appearance of $J^\pi = 4^-$ negative parity in the calculations of the psdpf, zbm model space at energy levels less than 10 MeV, while this level appears at energies greater than 10 MeV in the practical data, while at space model psd appeared at an energy level of 11 MeV, and thus it is in great agreement with the practical values, for psd space model, $J^\pi = 4^-$ appeared at an energy level of 11.989 MeV and is therefore in good agreement with the practical values[31].

The second sequence of spin appears $J^\pi = 2^-$ at the energy level of 7.343 MeV, 9.039 MeV of the zbm and psdpf model space respectively, while this amount appears at energy levels greater than 11 MeV at practical values Fig. (2). It is clearly observed by comparing these levels, that the fit of the values obtained from the virtues of the spsdpf model is better than values obtained from other space models, even at isospin T = 1 one can see that in Fig.(3). Through this agreement between theoretical and practical results, the shell model can be relied on to confirm some practically uncertain energy levels and can suggest some spin and parity values for energy levels certain but its spin and parity are undefined as shown in table 1, and Figs. (4,5).

When reviewing Table 1 clearly notice that many experimental values did not have comparable values within sd shell interactions, whose calculation was based on a new Hamiltonian [28], so it should be noted here that values close to the experimental values were obtained, and the difference between them is approximately 0.6 MeV or less, but the sequence is different, that is, in the reactions of the new USD , Theoretically have been getting an energy level of (9.806, 9.893, 9.93) MeV for Hamiltonian (USDB, USDC, USDCm), respectively whit $J^\pi = 2^+_4$ and was close to energy whit 9.284 MeV and $J^\pi = 2^+_5$. Almost every new Hamiltonian for sd gave a value of $J^\pi = 0^+_3$ at an energy level of 10.6 MeV while the other interactions psd, zbm, spsdpf were consistent with empirical $J^\pi = 0^+_4$ at an energy level of 10.11 MeV. Theoretical and experimental values very close, especially when the model space is expanded, and the difference appears only in the sequence of spin values of the sd shell.
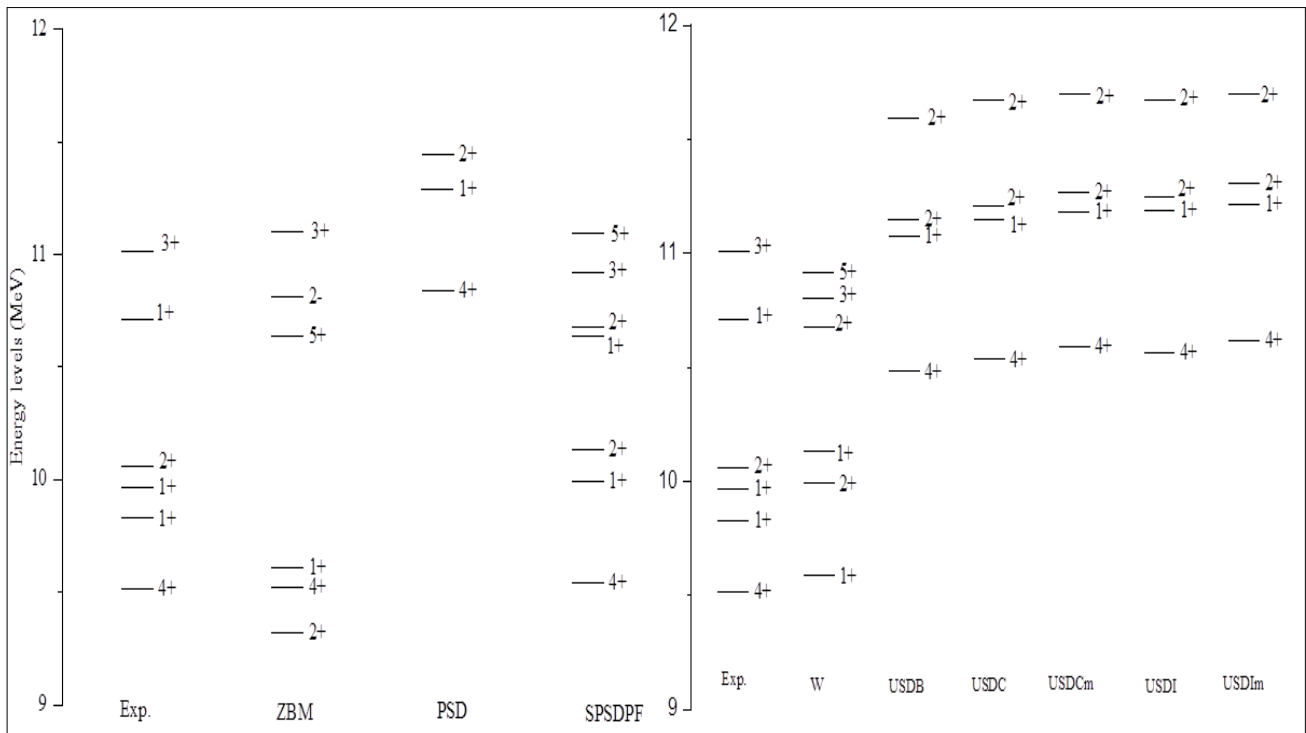
Figure 1. Comparing the energy level of the present work whit experimental values where isospin T=0 and for the First sequence.

| Experiment energy levels MeV	J^π	T isospin	Theory energy levels in MeV PRESENT WORK									J^π	sequence	certain & suggest values	
			zbm	psd	spsdpf	W	USDB	USDC	USDCm	USDI	USDIm				
9.2997	-------	0	9.77	----	9.315	----	----	------	-----	-----	------	3-	3	3-	suggest
9.3011	2+,3,4+	0	11	------	9.54	----	-----	------	-----	------	------	3-	4	3-	suggest
9.4578	(3)+	0	9.94	10.31	9.585	9.59	10.37	10.49	10.54	10.56	10.612	6+	2	6+	suggest
9.5162	(4+)	1	9.52	10.84	9.543	9.54	10.48	------	------	-----	10.617	4+	1	4+	certain
9.5278	(6+)	0	----	10.56	9.596	9.6	10.47	10.53	----	10.48	-----	3+	2	3+	suggest
9.5324	2+,3,4+	0	9.77	----	10.324	----	-----	-----	------	----	----	3-	5	3-	suggest
10.0585	(1,2)+	1	9.32	----	10.131	10.1	11.15	11.21	----	-----	-----	2+	1	2+	suggest
10.1109	----	0	10.1	11.14	10.678	10.7	11.06	11.19	11.25	11.33	11.383	0+	4	0+	suggest
10.3332	---	0	10.5	----	10.381	-----	-----	-----	-----	----	----	5-	2	5-	suggest
10.5813	2+,3,4+	0	11.1	-----	11.038	11	11.94	----	------	-----	12.156	4+	5	4+	suggest
10.6595	1,2+	0	----	----	11.819	11.8	12.83	-----	-----	----	12.972	2+	8	2+	suggest
10.6600	(4+)	0	----	---	10.623	----	---	----	-----	-----	----	5-	3	5-	suggest
10.8207	3+,4+	0	11.3	----	10.803	10.8	11.53	----	-----	----	11.632	3+	3	3+	suggest
11.0105	3	1	----	-----	12.191	12.2	----	-----	-----	----	----	3+	4	3+	suggest
11.1280	----	0	----	11.98	----	----	----	----	-----	-----	-----	4-	1	4-	suggest
11.1810	(3)-	0	10.3	----	10.13	----	-----	----	-----	-----	----	4-	2	4-	suggest
11.1868	----	0	----	----	11.579	11.6	----	----	----	----	----	3+	5	3+	suggest
11.2084	-----	0	11.5	----	11.134	----	----	-----	-----	----	----	4-	3	4-	suggest
11.2932	(2+,3,4+)	0	-----	-----	12.347	12.3	----	----	----	-----	----	3+	6	3+	suggest
11.3144	(3)+	0	11.7	-----	11.745	11.7	----	----	----	----	-----	4+	7	4+	suggest
11.3302	----	0	11.6	----	11.278	----	----	----	-----	----	----	4-	4	4-	suggest

Table 1. A comparison between practical and theoretical values to show agreement in the results and their adoption in confirming some values and suggesting others. The experimental data is taken from Ref [30].
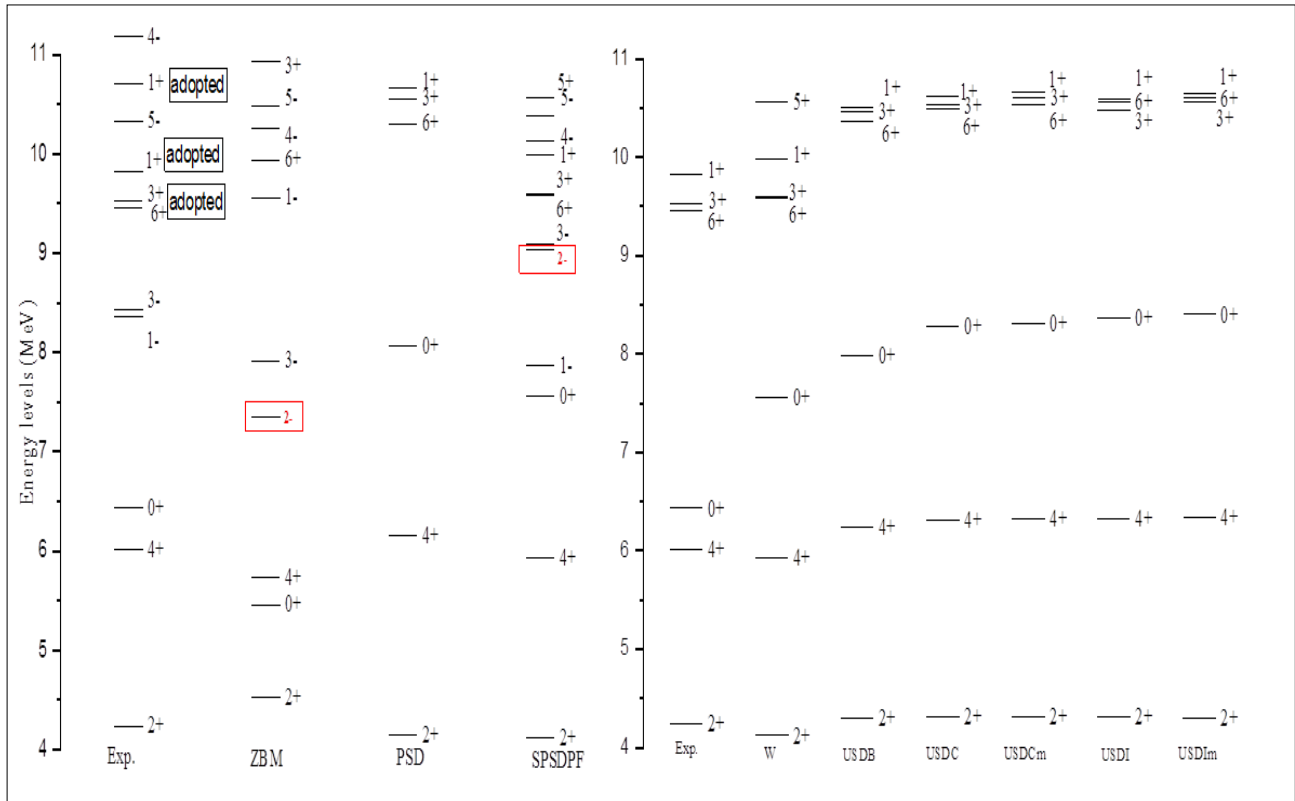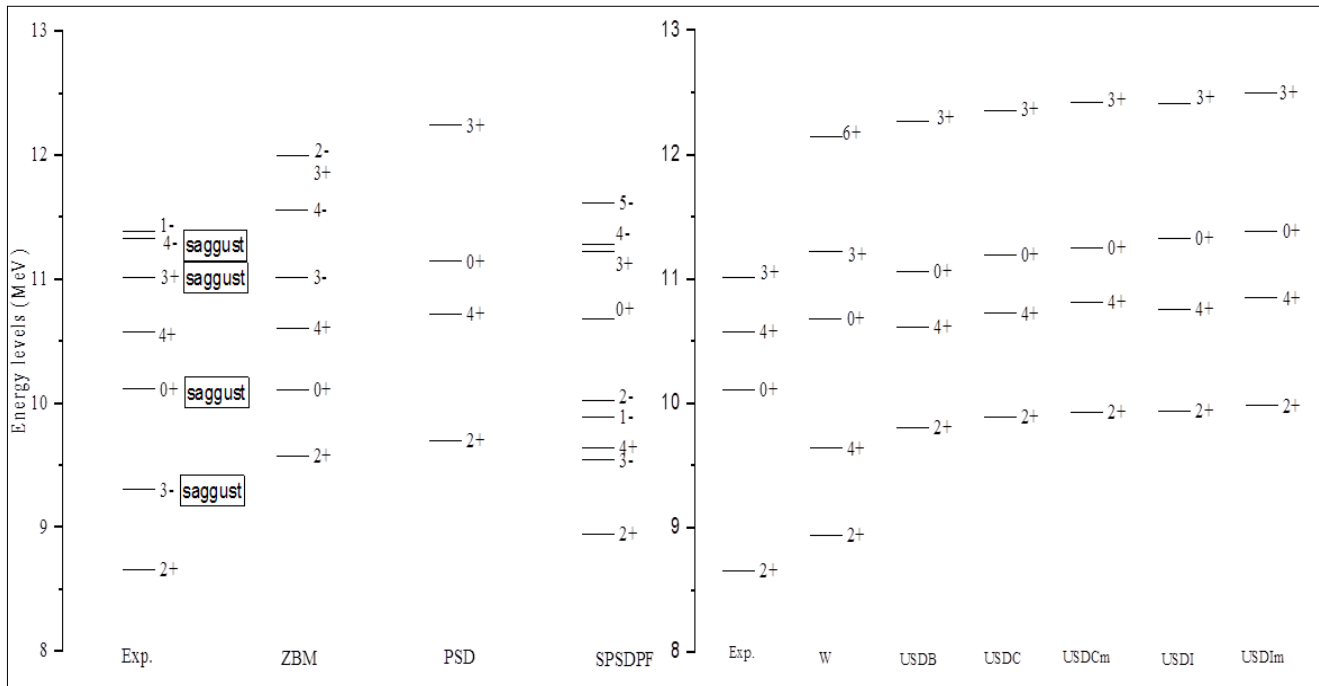
Figure 2. Comparing the energy level of the present work whit experimental values where T=0 and for the Second sequence.

Figure 3. Comparing the energy level of the present work whit experimental values where T=1 and for the First and Second sequence.
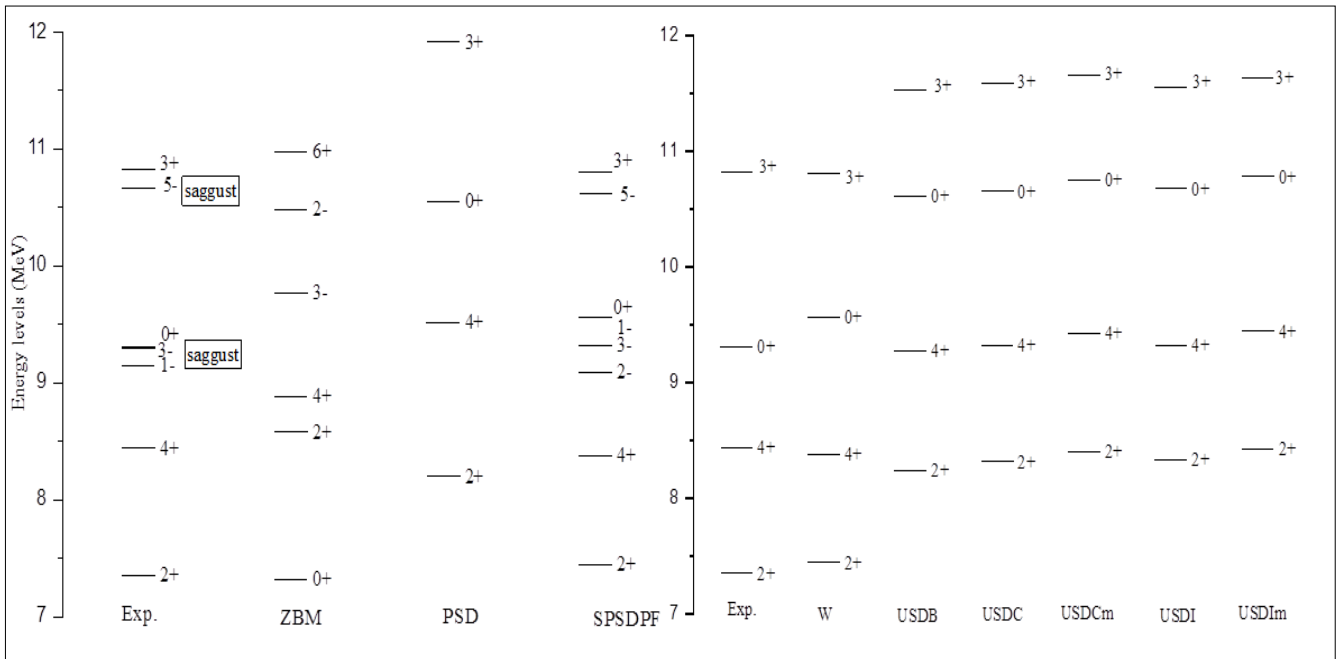
Figure 4. Comparing the energy level of the present work whit experimental values where T=0 and for the Third sequence.


Figure 5. Comparing the energy level of the present work whit experimental values where T=0 and for the fourth sequence.

b. Transverse form factors

Taken inelastic magnetic (M1, M3) and (M2, M4, M6) form factors of ^{24}Mg by depended on selection rules for electromagnetic transitions Eq.(11a, 11b) [32]

$$|J_i - J_f| \leqslant L \leqslant J_i + J_f \qquad (a)$$

$$\pi_i\,\pi_f = \begin{cases} (-1)^L & \text{for electric multipoles} \\ (-1)^{1+L} & \text{for magnetic multipoles} \end{cases} \quad (b) \right\} \qquad (11)$$

Figures 6,7, computed findings for inelastic magnetic form factors under consideration are plotted versus momentum transfer q and compared with experimental data for the transitions. It is crucial to note that transitions addressed in this work are $\Delta T = 1$. The transition from (G.S.) $J^\pi T = 0_1^+ 0$ to (E.S.) $J^\pi T = 1_1^+ 1$ at excited energy (E_x) = 9.966 MeV and $J^\pi T = 1_2^+ 1$ at E_x = 10.712 MeV in first and second sequence respectively plotted in Fig 6(a),7(a) as shown used different model space zbm, psd, spsdpf and one can see in Fig 6(b),7(b) that sd used two novel USD-type Hamiltonians, USDC and USDI, as well as modifications to these interactions, USDCm and USDIm [28]. It was found good garment between the calculated inelastic magnetic F_{M1}^2 and those of experimental data taken from Rf. [7], [13] [28].
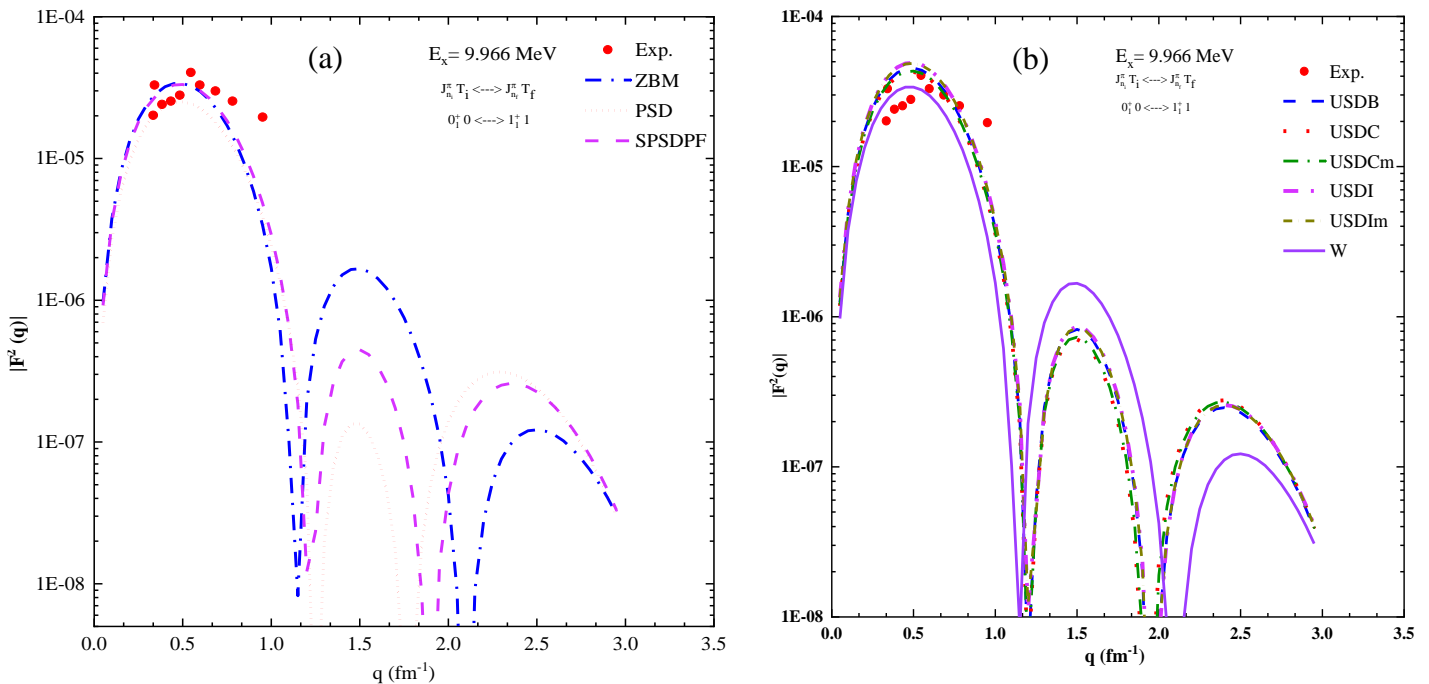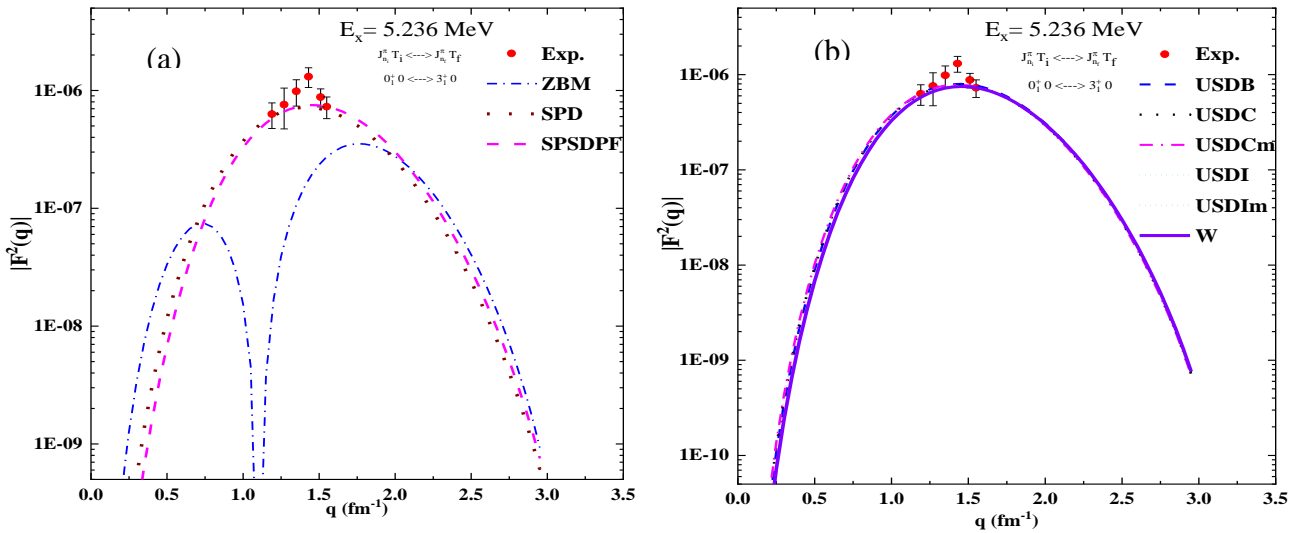

Figure 6. Comparing the results of transition form factor M1 for $0_1^+ 0 \rightarrow 1_1^+ 1$ **for the current work with the experimental data taken from the references [10][33] (a) Comparing of ZBM,PSD and SPSDPF model space with the experimental data (b) Comparing different interaction files of SD model space with experimental data.**
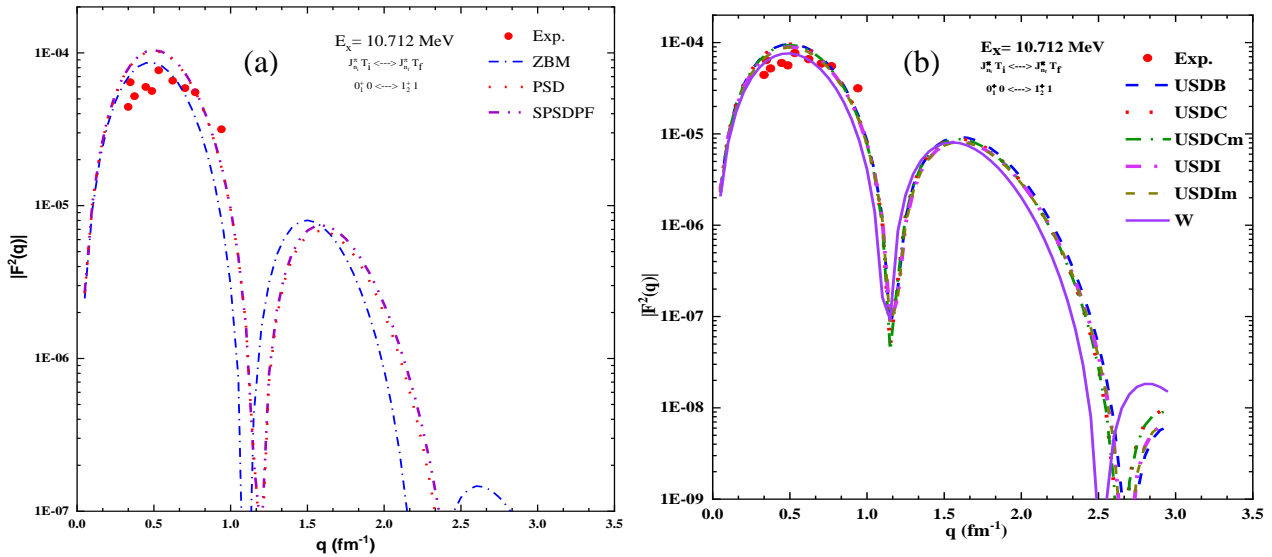
**Figure 8 represents comparison of the magnetic form factors of M3 whit the experimental**

data [34]. The transition from G.S. JπT= 0_1^+0 to E.S. $J^\pi T = 3_1^+0$ at excited energy Ex = 5.236 MeV , the calculation was made with a change in the g factors values, the values were $g_l^p = 1.060$ and $g_l^n = -0.060$. There is an acceptable agreement between the current accounts and the available practical values. psd, spsdpf and sd gave a better affinity than what is observed at the model space ZBM, which may indicate the weak transfer of particles at this energy within this model, and this is contrary to what was seen in the lower energy level in the previous figs. 6,7.

Figure 8. Comparing the results of transition form factor M3 for $0_1^+0 \rightarrow 3_1^+1$ for the current work with the experimental data taken from the references [34] (a) Comparing of ZBM,PSD and SPSDPF model space with the experimental data (b) Comparing different interaction files of SD model space with experimental data.

Figure (9-12) the negative parity of the transitions was taken. Transitions from the ground level (0.000)MeV to the (E_x= 12.640, 12.700, 13.370) MeV which given M2 magnetic transition form factor and (E_x= 15.540, 15.130) MeV for M4, M6 respectively. It was based on the values of the changed g-factors as previously indicated $g_l^p = 1.060$ and $g_l^n = -0.060$.

Figure 9(a) shows the. Note that the values of momentum transfers q for practical values located at 1≤ q ≤ 2 while this study shows 0.5≤ q ≤ 1.5. Perhaps this disparity is due to the effect of the residual potential of the interaction between particles referred to in the reference [35], where the default potential of the Oxbash code was applied. Fig. 9(b) plotted the form factor for M2, transition to second sequence of state $J^\pi T = 2_2^- 1$, at Ex = 13.370 MeV, one can   note   the 0.5≤ q ≤ 1 For current study and practical values.
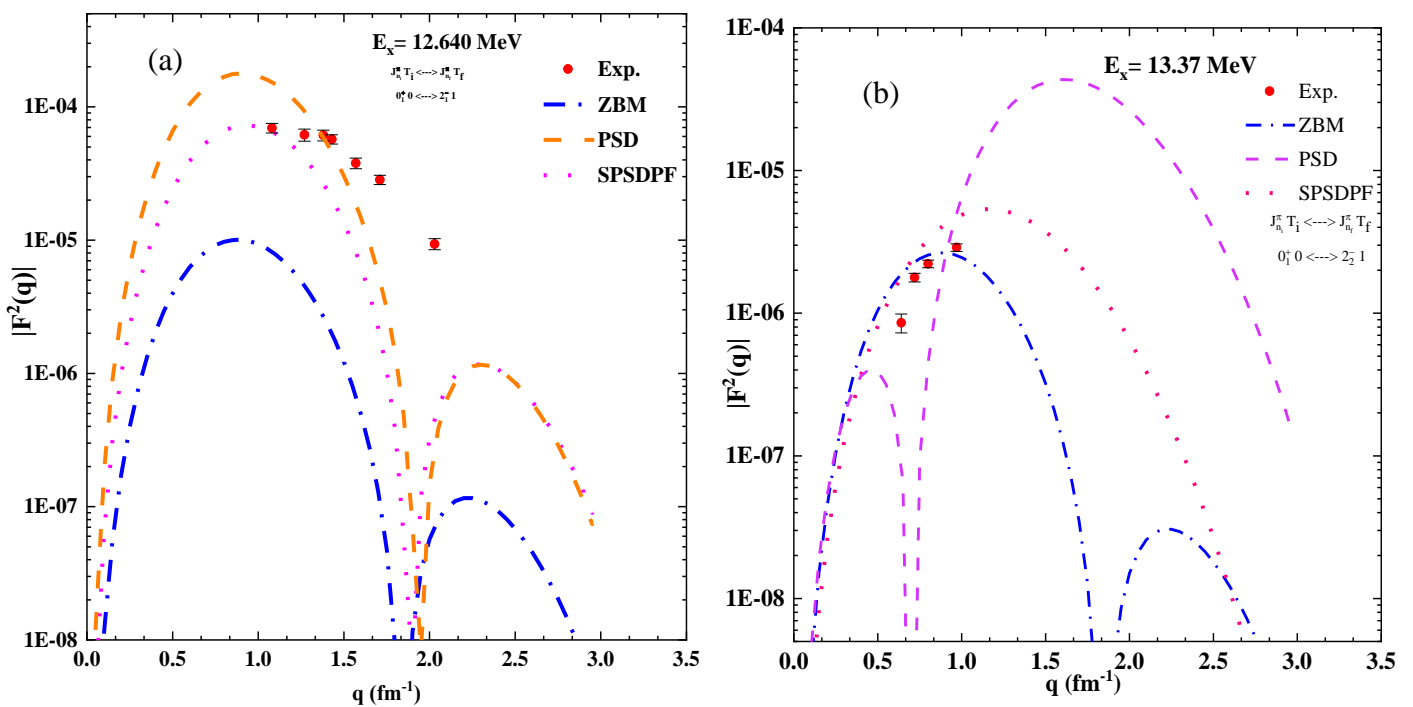
Figure 9. Comparing the results of transition form factor M2 from negative parity for ZBM,PSD and SPSDPF model space with the experimental data taken from the references [34] (a) transtion for $0_1^+ 0 \rightarrow 2_1^- 1$ (b) transtion for $0_1^+ 0 \rightarrow 2_2^- 1$.

The magnetic form factor M2 transitions from G.S. $J^\pi T = 0_1^+ 0$, to Ex = 12.70 MeV

it spin $J^\pi T = 2_2^- 0$, shown in Fig.10. When constructing the wave function and the eigenvalue of the model space. The SPSDPF model space show greater contribution and agreement with experimental values, the number of freedoms of the number of particles transferred to a high state is restricted by applying the constraint $0,1\hbar w$ this is to reduce the number of configurations than if they were left unrestrained and therefore require more time and storage space to complete the calculations.

It can be said that the theoretical calculations at isoscalar show a better agreement with the experimental values than these was seen with isovector at excite energy greet then 14MeV, as shown in Figs. (11, 12).
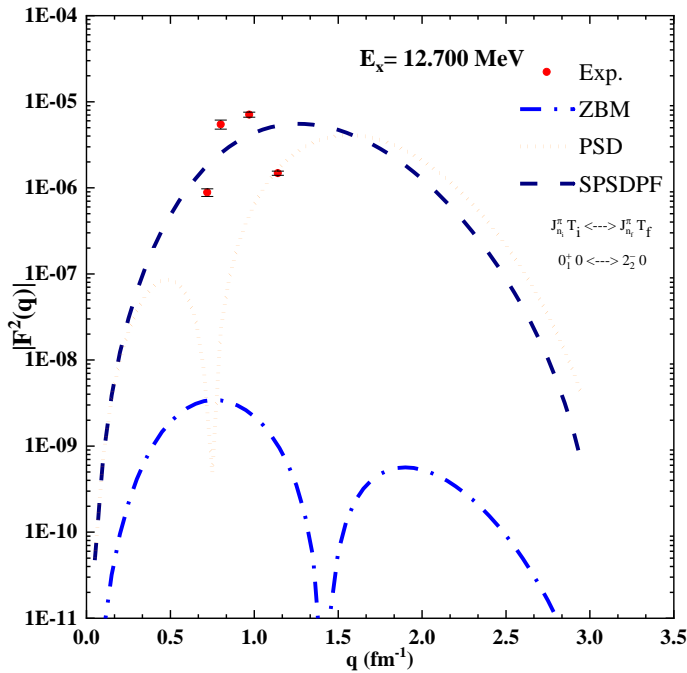

Figure 10. Comparing the results of transition form factor M2 from negative parity $0_1^+0 \rightarrow 2_2^-0$ **for ZBM,PSD and SPSDPF model space with the experimental data taken from the references [10]**
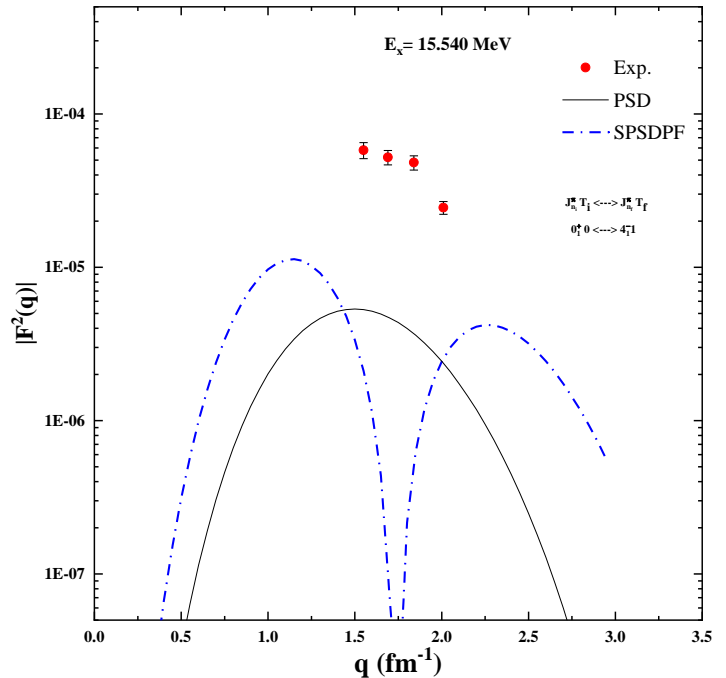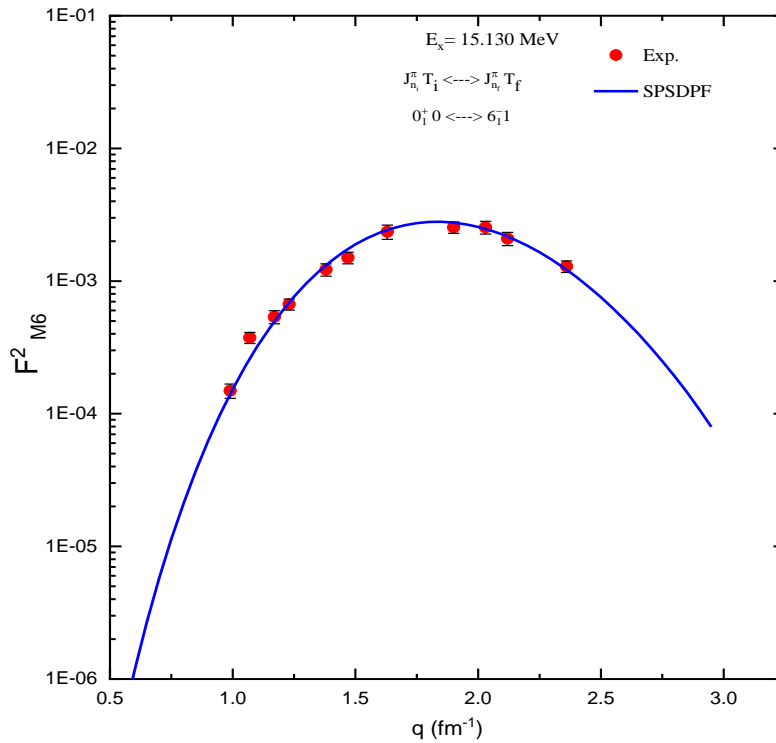

Figure 11. Comparing the results of transition form factor M4 from negative parity $0_1^+0 \rightarrow 4_1^-1$ **for ,PSD and SPSDPF model space with the experimental data taken from the references [36]**

The contribution of (M4) at E_x= 15.540 MeV, $J^\pi T = 4_1^-1$ appears the magnetic form factor $|F_{M4}(q)|^2$ less than what was found experimentally but is well agreed to the values of $q \approx 1.5$ fm^{-1} see Fig. 11.

Diagram in Fig.12 shows the transition from the G.S. to the Ex= 15.130 MeV 1st sequence of spin $J^\pi T = 6_1^-1$. The significant agreement in the value of (q) for the calculated experimental and theoretical results, is noticed in the value of $|F_{M6}(q)|^2$. In the experimental research, the researcher [36] referred to the use of the scattering angle of 160 while the oxbash code is calculated by assuming an angle of 90, so the change in the angle has been by Eq. $F^2 = FLONG^2 + [0.5 + TAN^2(THETA/2)] * (FTRANS^2)$ to get on this the good result, where $(FLONG^2)$ is longitudinal form factor and $(FTRANS^2)$ is transver form factor.

Figure 12. Comparing the results of transition form factor M6 from negative parity $0_1^+0 \rightarrow 6_1^-1$ **for SPSDPF model space with the experimental data taken from the references [36]**

3. Conclusion

This study shows a comparison of the calculated energy levels of the ^{24}Mg structure as well as the magnetic formation factor ML with the available experimental data. Good results for energy levels were obtained when using the new Hamiltonians (USDC, USDCm, USDI, and USDIm), which showed some experimentally uncertain energy levels that could be considered to be confirmed. The model space was taken as expanded, unlike the usual, where the model space zbm, psd, and spsdpf was entered in order to include negative parity within the calculations, which showed more information about the nucleus structure. By introducing negative parity, it was allowed to study the magnetic form factor for the even values of ML as in M2, M4, and M6.

The computation values, after comparing them with the experimental data, showed the importance of the transition at the isovector and isoscalar, especially at the regions $q > 2 \, mf^{-1}$, changing the effective g values is an important tool for describing the magnetic transition and was more effective at the magnitude $g_l^p = 1.060$ and $g_l^n = -0.060$

References

[1] B. A. Brown, "Towards the future of the nuclear shell model," *Nucl. Phys. A*, vol. 704, no. 1–4, pp. 11–20, Jun. 2002.

[2] N. M. Adeeb, A. A. Alzubadi, and O. A. Jalal, "Longitudinal and Transverse Electron Scattering Form Factors for 13 C Nucleus with Core-Polarization Effects," *Iraqi J. Sci.*, vol. 54, no. 4, pp. 888–894, 2013.

[3] K. S. Jassim, A. A. Al-Sammarrae, F. I. Sharrad, and H. Abu Kassim, "Elastic and inelastic electron-nucleus scattering form factors of some light nuclei: Na 23, Mg 25, Al 27, and Ca 41," *Phys. Rev. C*, vol. 89, no. 1, pp. 1–9, 2014.

[4] A. A. T. Aldalawi, M. Y. Hadi, and R. A. Hameed, "Calculate Effective Atomic Number, Mass and Cross-Section Attenuation Coefficients for Nonanoic Acid by Using Gamma-Ray Sources," *NeuroQuantology*, vol. 19, no. 11, p. 15, 2021.

[5] M. Y. Hadi, A. A. T. Aldalawi, and K. M. Talib, "Study Total Atomic Cross-Sections, Effective Atomic Numbers, and Electron Densities for Palmitic Acid by Using Sources of Gamma Ray," *NeuroQuantology*, vol. 19, no. 9, p. 152, 2021.

[6] M. Y. Hadi, A. H. F. Alnasraui, and A. A. T. Aldalawi, "Measurement Mass Attenuation Coefficient of Palmitic Acid by Using Sources of Gamma Ray," *NeuroQuantology*, vol. 19, no. 6, p. 107, 2021.

[7] A. A. Al-Sammarraie, F. I. Sharrad, and H. A. Kassim, "Nuclear structure for 24 Mg within sd-shell model space Hamiltonians," *Armen. J. Phys.*, vol. 8, no. 4, pp. 170–179, 2015.

[8] L. Vinet and A. Zhedanov, "Lecture Notes in Nuclear Structure Physics," *Antimicrob. Agents Chemother.*, pp. 1–290, Nov. 2010.

[9] J. B. M. Cgrory2 and B. H. W. Ildenthal3, "LARGE SCALE SHELL MODEL CALCULATIONS," 1980.

[10] A. Johnston and T. E. Drake, "A study of 24Mg by inelastic electron scattering," *J. Phys. A Gen. Phys.*, vol. 7, no. 8, pp. 898–935, 1974.

[11] A. A. Al-Sa'ad and A. A. Abbass, "Core-polarization effects on the isovector magnetic dipole transitions in 24Mg," *Chinese J. Phys.*, vol. 50, no. 5, pp. 768–775, 2012.

[12] P. J. Davies *et al.*, "Toward the limit of nuclear binding on the N=Z line: Spectroscopy of Cd 96," *Phys. Rev. C*, vol. 99, no. 2, 2019.

[13] O. Titze, "Unelastische Elektronenstreuung an24Mg bis 11,5 MeV Anregungsenergie," *Zeitschrift für Phys.*, vol. 220, no. 1, pp. 66–85, 1969.

[14] A. A. Al-Sammarraie, F. A. Ahmed, and A. A. Okhunov, "Large scale shell model calculations of the negative-parity states structure in 24Mg nucleus," *Ukr. J. Phys.*, vol. 66, no. 4, pp. 293–302, 2021.

[15] T. W. Donnelly and I. Sick, "Elastic magnetic electron scattering from nuclei," *Rev. Mod. Phys.*, vol. 56, no. 3, pp. 461–566, Jul. 1984.

[16] Igor A. Zaliznyak and Seung-Hun Lee, "MAGNETIC NEUTRON SCATTERING. And Recent Developments in the Triple Axis Spectroscop," *Neutron Scatt. from Magn. Mater.*, no. 1, pp. 1–24, 2006.

[17] L. J. Tassie and F. C. Barker, "Application to electron scattering of center-of-mass effects in the nuclear shell model," *Phys. Rev.*, vol. 111, no. 3, pp. 940–1, 1958.

[18] B. A. Brown *et al.*, "Shell-model analysis of high-resolution data for elastic and inelastic electron scattering on F19," *Phys. Rev. C*, vol. 32, no. 4, pp. 1127–1156, Oct. 1985.

[19] T. de Forest and J. D. Walecka, *Electron scattering and nuclear structure*, vol. 15, no. 57. 1966.

[20] C. F. Perdrisat, V. Punjabi, and M. Vanderhaeghen, "Nucleon electromagnetic form factors," *Prog. Part. Nucl. Phys.*, vol. 59, no. 2, pp. 694–764, 2007.

[21] H. Chandra and G. Sauer, "Relativistic corrections to the elastic electron scattering from Pb208," *Phys. Rev. C*, vol. 13, no. 1, pp. 245–252, Jan. 1976.

[22] A. A. Al-Sammarraie, F. I. Sharrad, N. Yusof, and H. A. Kassim, "Longitudinal and transverse electron-nucleus scattering form factors of Mg 25," *Phys. Rev. C*, vol. 92, no. 3, pp. 1–14, 2015.

[23] B. A. Brown, A. Etchegoyen, W. D. M. Rae, and N. S. Godwin, "The computer code OXBASH," *MSU-NSCL Report*, vol. 524. 1988.

[24] S. Mohammadi, S. H. Rostami, A. R. Mohasel, M. Ghamary, and A. Rashed Mohasel, "Energy Levels Calculations of 36-37-38 Ar Isotopes Using Shell Model Code OXBASH," *Am. J. Mod. Physics. Spec. Issue Many Part. Simulations*, vol. 4, no. 1, pp. 23–26, Mar. 2015.

[25] R. A. Radhi, N. T. Khalaf, and A. A. Najim, "Elastic magnetic electron scattering from 17O, 25Mg and 27Al," *Nucl. Phys. A*, vol. 724, no. 3–4, pp. 333–344, Sep. 2003.

[26] M. Y. Hadi and A. A. Al-Sa'ad, "Calculations of the Shell Model for 27Mg Isotope," *J. Kufa-Physics*, vol. 15, no. 01, pp. 37–45, Jun. 2023.

[27] M. Y. Hadi and A. A. Al-sa'ad, "Nuclear Structure of Proton-rich 20-23Mg Isotopes," *Acta Phys. Pol. B*, vol. 54, no. 1, pp. 1–16, 2023.

[28] A. Magilligan and B. A. Brown, "New isospin-breaking 'USD' Hamiltonians for the sd shell," *Phys. Rev. C*, vol. 101, no. 6, pp. 1–15, 2020.

[29] B. A. Brown and W. A. Richter, "New 'USD' Hamiltonians for the sd shell," *Phys. Rev. C*, vol. 74, no. 3, pp. 1–11, 2006.

[30] R. B. Firestone, "Nuclear Data Sheets for A = 24," *Nucl. Data Sheets*, vol. 108, no. 11, pp. 2319–2392, 2007.

[31] National Nuclear Data Center NNDC, "List of levels for 24Mg," *https://www.nndc.bnl.gov/ensdf/*, 2007. .

[32] P. J. Brussaard and P. W. M. Glaudemans, *Shell-model applications in nuclear spectroscopy*. Elsevier, 1977.

[33] B. A. Brown and B. H. Wildenthal, "Strengths of transitions between 0+ and 1+ states and their relationship to inelastic electron scattering form factors: Example of Mg24," *Phys. Rev. C*, vol. 27, no. 3, pp. 1296–1301, 1983.

[34] I. J. D. Macgregor, A. Johnston, and J. S. Ewing, "Electron scattering measurements of inelastic M3 transitions," *Nucl. Phys. A*, vol. 412, no. 1, pp. 1–12, 1984.

[35] A. Polls, A. Ramos, and H. Müther, "Effective interaction for the shell model in the 1p0f shell," *Nucl. Phys. A*, vol. 518, no. 3, pp. 421–440, 1990.

[36] H. Zarek *et al.*, "Inelastic electron scattering to negative parity states of Mg24," *Phys. Rev. C*, vol. 29, no. 5, pp. 1664–1671, 1984.